Light regulation of type IV pilus-dependent motility by chemosensor-like elements in *Synechocystis* PCC6803

Devaki Bhaya*†, Akiko Takahashi‡, and Arthur R. Grossman*

*Department of Plant Biology, The Carnegie Institution of Washington, Stanford, CA 94305; and ‡Laboratory for Metabolic Compartmentation, The Institute of Physical and Chemical Research, Plant Science Center, 2-1 Hirosawa, Wako, Saitama, 351-0198 Japan

Communicated by Winslow R. Briggs, Carnegie Institution of Washington, Stanford, CA, April 23, 2001 (received for review March 12, 2001)

To optimize photosynthesis, cyanobacteria move toward or away from a light source by a process known as phototaxis. Phototactic movement of the cyanobacterium *Synechocystis* PCC6803 is a surface-dependent phenomenon that requires type IV pili, cellular appendages implicated in twitching and social motility in a range of bacteria. To elucidate regulation of cyanobacterial motility, we generated transposon-tagged mutants with aberrant phototaxis; mutants were either nonmotile or exhibited an ''inverted motility response'' (negative phototaxis) relative to wild-type cells. Several mutants contained transposons in genes similar to those involved in bacterial chemotaxis. *Synechocystis* PCC6803 has three loci with chemotaxis-like genes, of which two, *Tax1* and *Tax3*, are involved in phototaxis. Transposons interrupting the *Tax1* locus yielded mutants that exhibited an inverted motility response, suggesting that this locus is involved in controlling positive phototaxis. However, a strain null for *taxAY1* was nonmotile and hyperpiliated. Interestingly, whereas the C-terminal region of the TaxD1 polypeptide is similar to the signaling domain of enteric methyl-accepting chemoreceptor proteins, the N terminus has two domains resembling chromophore-binding domains of phytochrome, a photoreceptor in plants. Hence, TaxD1 may play a role in perceiving the light stimulus. Mutants in the *Tax3* locus are nonmotile and do not make type IV pili. These findings establish links between chemotaxis-like regulatory elements and type IV pilus-mediated phototaxis.

Swimming of bacteria in liquid by means of flagella is well characterized. Gliding and twitching motility on solid surfaces are less well understood forms of locomotion exhibited by many Gram-negative bacteria (1, 2). This mode of slow translocation usually requires surface appendages known as type IV pili (Tfp), which are defined by structural, morphological, and antigenic properties (3). The capacity of Tfp to retract or extend may enable cells to move (4). There is also growing evidence that Tfp are multifunctional, participating in a variety of processes including transformation competence, secretion, and attachment to host receptors (5, 6).

Tfp biogenesis has been studied in *Myxococcus xanthus* and the pathogenic microorganisms *Pseudomonas aeruginosa*, *Neisseria gonorrhoeae, Vibrio cholerae*, and enteropathogenic *Escherichia coli*. Whereas genes required for Tfp biogenesis have been identified in these organisms (7–10), little is understood about the regulation of Tfp biogenesis. Social motility in *M. xanthus* appears to require chemotaxis-like genes (*che* genes encoding Che polypeptides); their exact role in regulating this process is unclear (11–13).

Limited aspects of motility have been described for cyanobacteria (14, 15). Filamentous gliding cyanobacteria, major components of microbial mats and biofilms, require contact with a solid surface and, in certain species, the extracellular glycoprotein, oscillin, for motility (16). An outer membrane protein with features similar to that of oscillin is required for swimming of the marine cyanobacterium *Synechococcus* WH8102 (17).

Recent studies have demonstrated that the cell surface of the freshwater unicellular cyanobacterium *Synechocystis* PCC6803 (*Synechocystis* throughout) has a dense covering of pilus-like appendages of two distinct morpho-types. The thick pilus morpho-type (6–8 Å in diameter) is required for motility and represents Tfp (18). The thin pilus morpho-type (3–4 Å in diameter) is shorter than Tfp and uniformly covers the cell surface. The function(s) of thin pili are not known.

Light is a key environmental cue that regulates cyanobacterial motility. Cyanobacteria, as well as other photosynthetic bacteria, exhibit at least three movement responses relative to light: phototaxis [orientation of cells with respect to the direction of light and subsequent movement either toward (positive) or away (negative) from the light], photophobic movement, and photokinesis (14, 19). We have recently isolated numerous mutants with aberrant phototactic movement. Several of the mutants harbored transposons in *che*-like genes, which are well studied with respect to flagellar-based movement but have only recently been implicated in controlling Tfp-based motility (12, 13, 20). The phenotypes of the phototaxis mutants suggest that Che-like polypeptides control both cell orientation with respect to light and pilus biosynthesis.

Experimental Procedures

Culture and Growth Conditions and Motility Assays. The motile strain of *Synechocystis* was grown in BG-11 medium in light of 50–70 μmol photons m^{-2} s^{-1}. When appropriate, antibiotics were included in the medium at a final concentration of 25 μg/ml spectinomycin, 10 μg/ml kanamycin, or 25 μg/ml chloramphenicol. Motility was assayed with incandescent light (intensity at the colony surface $\approx$40 μmol photons m^{-2} s^{-1}), as previously described (18).

DNA Manipulation, RNA Isolation, and RNA Hybridization Analysis. Molecular techniques were performed according to standard procedures (21), and RNA was isolated as described (22).

Genomic Library Preparation, Transposon Mutagenesis, and Direct Genomic Sequencing. A *Synechocystis* genomic library was constructed that contained 10^5 clones with inserts of 4–9 kbp (23). The library was subjected to *in vitro* transposon mutagenesis (protocol of Epicentre Technologies, Madison, WI) and then transformed into wild-type *Synechocystis* cells. Following transformation, cells were spread on 0.4% or 0.6% BG-11 agar plates (10 μg kanamycin/ml) and placed in a directional light source. Colonies that were nonmotile or exhibited an inverted response were picked and rescreened. To define the transposon insertion

Abbreviation: Tfp, type IV pili.

†To whom reprint requests should be addressed. E-mail: devaki@andrew2.stanford.edu.

The publication costs of this article were defrayed in part by page charge payment. This article must therefore be hereby marked "*advertisement*" in accordance with 18 U.S.C. §1734 solely to indicate this fact.

www.pnas.org/cgi/doi/10.1073/pnas.131201098

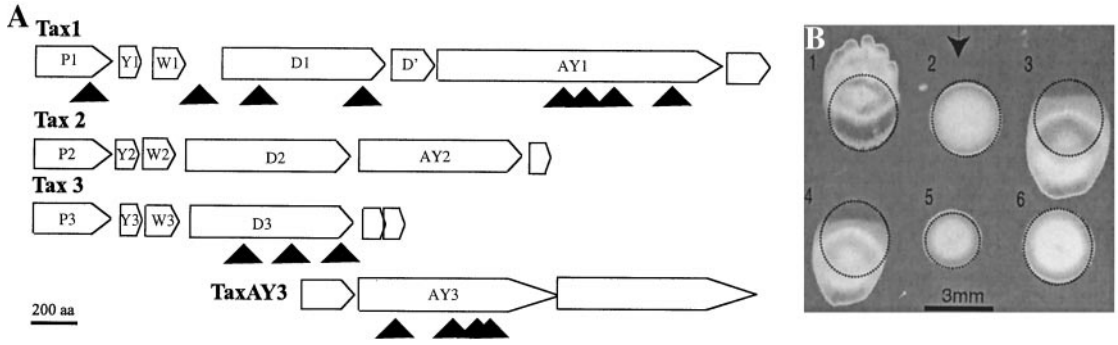

Fig. 1. (*A*) Physical map of *Tax* loci showing three *Tax* loci (*Tax1*, *Tax 2*, and *Tax3*) and *taxAY3*. Arrowheads indicate the position of transposons that map to specific *tax* genes. (Bar, 200 amino acids or 600 nucleotides.) (*B*) Directional motility assays. Cells were spotted (shown by dotted circle) onto 0.4% agar plates and placed in a directional light source (arrowhead) for 3 days. *1*, wild-type; *2*, *taxAY1-5′*; *3*, *taxAY1-3′*; *4*, *taxD1*; *5*, *taxAY3*; and *6*, the *taxD3* transposon mutant.

site, genomic DNA was isolated from mutants by using the QIAGEN DNA Easy Kit, and purified DNA was sequenced from the transposon borders with ABI Big Dye Cycle Sequencing Ready Reaction Kit (Perkin–Elmer) and RP1 or FP1 primers (Epicentre Technologies). Sequence information identified the site of the transposon insertion (Cyanobase, http://www.kazusa.or.jp/cyano/).

Gene Inactivations. Genes of interest were amplified (using specific primers) from genomic DNA by using High Fidelity *Taq* polymerase (Roche Molecular Biochemicals), cloned into the pGEM-T vector (Promega), and disrupted with an antibiotic marker cassette; plasmid DNA containing the interrupted gene was then transformed into *Synechocystis* (18). For inactivation of *taxAY1* at the 5′ end (mutant *taxAY1*-5′), the gene was amplified by PCR (primers 5′-ATGCTCAACTCCGACATT and 5′-TTAACTGCTGACCGATAA), cloned into pGEM-T vector, and disrupted by excising an internal, 3.41-kbp *Bgl*II fragment from the coding region of the gene and replacing the fragment with a cassette conferring chloramphenicol resistance. To inactivate *taxAY1* at the 3′ end, in the region encoding the CheY-like domain (mutant *taxAY1*-3′), a PCR fragment was generated using primers 5′-TTGACCGCCGATGAACTG and 5′-CAGTTCATCGGCGGTCAA to amplify a 2.17-kbp fragment. A cassette conferring spectinomycin resistance was ligated into the unique *Bgl*II site of this fragment. The *taxD1* gene was PCR amplified using primers 5′-ATGGCAGAGGCTTTTATAGCA and 5′-TCACTGCACTTTGAACTG and cloned into the pGEM-T vector. For inactivation of *taxD1*, a cassette conferring spectinomycin resistance was ligated into the unique *Sma*I site of the 2.68-kbp PCR fragment cloned into pGEM-T vector. The *taxAY3* gene was amplified with the primers 5′-ATGACTAGCGATCCCAAT and 5′-TTACTCGTCTGCTGCACTTAG and cloned into the pGEM-T vector. An inactivation that would disrupt the protein at the N terminus was created by insertion of the spectinomycin cassette into a unique *Eco*RI site.

Vectors containing the gene disruptions were transformed into *Synechocystis* by selecting for antibiotic resistance (22). Genomic DNA from transformants was isolated and analyzed by PCR to ensure that all chromosomal copies of the targeted gene were disrupted.

Electron Microscopy. Electron microscopy was performed with a Phillips CM410 microscope, as described (18).

Results

Cells were mutagenized by *in vitro* transposon mutagenesis, and 300 motility mutants from 8,000 transformants were identified. Ninety percent of these were nonmotile, whereas 10% exhibited an inverted motility response (or negative phototaxis) relative to wild-type cells. To identify sites of transposon insertions, we sequenced genomic DNA using primers that anneal to the ends of the transposon–kanamycin cassette. Many genes required for pilus biogenesis or function were identified, including those encoding polypeptides with a coiled coil structure, chaperones, and ABC transporters (refs. 10, 24, and 25; D.B. and A.R.G, unpublished results). Several mutants harbored insertions in genes encoding Che-like polypeptides; these polypeptides control flagellar-based movement of bacteria in response to environmental signals.

The genome of *Synechocystis* contains three loci encoding putative Che-like proteins. Each locus, designated *Tax1*, *Tax2*, and *Tax3*, contains a cluster of genes arranged in a similar manner (Fig. 1*A*). The *Tax* designation is more general than that of *Che* and reflects the finding that genes within two of the *Synechocystis* loci are involved in photo*tax*is. The *Tax1* locus has six ORFs (Cyanobase designation sll0038–sll0043) ordered *taxP1-taxY1-taxW1-taxD1-taxD′-taxAY1*. The *Tax2* locus has five ORFs (sll1291–sll1295) ordered *taxP2-taxY2-taxW2-taxD2-taxAY2*. The *Tax3* locus has four ORFs (slr1041–slr1045) ordered *taxP3-taxY3-taxW3-taxD3*. A separate *taxAY* gene (sll0322), designated *taxAY3* (based on the phenotype of the mutant strain; see below), is located in another region of the chromosome. Specific ORFs not similar to known Che proteins, but included in Fig. 1*A*, are immediately downstream and in the same orientation on the genome as the *tax* genes: sll0044 in the *Tax1* locus, sll1297 in the *Tax2* locus, and slr1046/1047 in the *Tax3* locus. We have given a *taxP* designation to the first gene in each of the three *Tax* loci because these putative *taxP* genes encode polypeptides that are ≈25% identical (40% similar) to each other and contain C-terminal sequences similar to the regulatory CheY protein (about 33% identity and 52% similarity). Also, one of the inverted response mutants contained a transposon in *taxP1*, suggesting a function for TaxP1 in motility. TaxP polypeptides are part of a family of proteins in *Synechocystis*, with at least three other homologs encoded on the genome (slr1693, slr1214, and slr1594). They show homology to PatA, which is involved in heterocyst development and pattern formation in the nitrogen-fixing cyanobacterium *Anabaena* (26).

Of the 50 mutants analyzed, transposons in 15 were localized to *Tax* loci (Fig. 1*A*). Insertions in *taxP1*, *taxD1*, *taxAY1*, and between *taxW1* and *taxD1* were identified in strains with an inverted response phenotype. All of the insertions within *taxAY1* were in the 3′ end of the gene (nucleotide positions 2174, 2475, 2941, and 3670), which would disrupt the C-terminal portion of the polypeptide. All seven strains disrupted for *taxAY3* and *taxD3* were nonmotile.

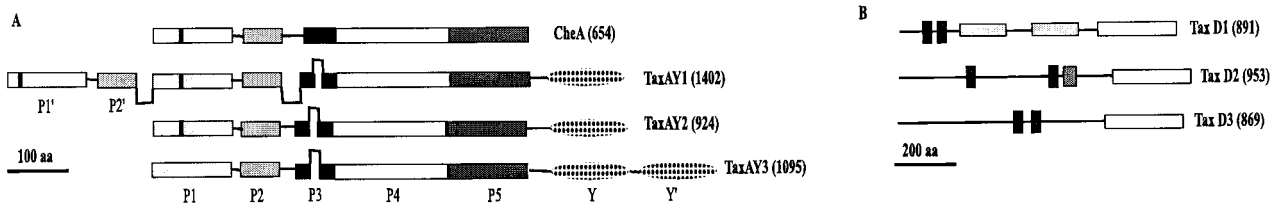

Fig. 2. (*A*) Diagram of TaxAY histidine kinases showing the different domains (P1–P5) and the CheY-like domains (dotted boxes). CheA from *E. coli* is shown in line 1; numbers in parentheses represent protein size in amino acids. Black bar in P1 represents the H box. (*B*) Diagram of TaxD chemosensor-like polypeptides showing putative transmembrane helices (black bars), phytochrome-like domains in TaxD1 (gray boxes), and signaling domains (white boxes). The HAMP domain of TaxD2 is shown as a dark gray box. Numbers in parentheses represent protein size in amino acids.

To confirm transposon mutant phenotypes, we insertionally inactivated *taxD1*, *taxAY1*, *taxD2, taxAY2*, and *taxAY3*. Furthermore, because the transposons only disrupted *taxAY1* at its 3′ end, possibly not resulting in a null mutation, we introduced individual targeted insertions into the 3′ and 5′ ends of the *taxAY1* coding region. The motility of these strains is shown in Fig. 1*B*. The *taxAY1*-3′ and *taxD1* mutants exhibited an inverted response (Fig. 1*B*, 3 and 4). In contrast, the *taxAY1*-5′ mutant exhibited a nonmotile phenotype (Fig. 1*B*, 2), suggesting two separable activities associated with the TaxAY1 protein. Distinct phenotypes of cyanobacterial strains with 5′ and 3′ disruptions of *rcaE*, which encodes a sensor that controls the responses of a filamentous cyanobacterium to light quality, have also been noted (27).

No transposon insertions in the *Tax2* locus were identified in the mutant collection. Furthermore, targeted disruption of *taxD2* or *taxAY2* caused no marked change in the motility of the cells (data not shown).

Seven transposon insertions within the *taxAY3* and *taxD3* genes yielded nonmotile mutants (Fig. 1*B*, 5 and 6), which was confirmed by a targeted inactivation of *taxAY3* (at the 5′ end). Although a gene encoding an α-mannosidase (sll0323) is located downstream of *taxAY3*, it is unlikely that the nonmotile phenotype is caused by a downstream polar effect, as both the kanamycin cassette (which has no terminator) and the targeted inactivation yielded a nonmotile phenotype.

The domain structure of the putative TaxAY polypeptides is shown in Fig. 2*A* (for a detailed comparison of TaxAY polypeptides see ftp://carnegiedpb.stanford.edu/pub/TaxAY-comparisons.pdf). All three of the *Synechocystis taxA* genes encode histidine kinases fused at their C termini to CheY-like domains; TaxAY3 has two CheY-like domains. The fused CheY-like domains are homologous to each other and to the independent, putative CheY-like polypeptides encoded by *taxY1*, *taxY2*, and *taxY3* (≈30% identity and 50% similarity). In addition, all have the highly conserved aspartate that undergoes phosphorylation. The P1 domain, which contains the autophosphorylatable histidine, is well conserved in TaxAY1 and TaxAY2 but not in TaxAY3; TaxAY3 appears to completely lack the H box. Interestingly, TaxAY1 contains a duplication of the P1 and P2 domains (P1′ and P2′) and also contains a glutamate/proline-rich insertion of 140 aa between P2 and the dimerization domain (P3). The P2 domain, presumed to interact with CheY, shows moderate homology among the TaxAY polypeptides and CheA from *E. coli*. The P3 domain is also conserved among TaxAY polypeptides and *E. coli* CheA, although the TaxAY polypeptides have a ≈70-aa insertion within this domain. The P4 and P5 domains, required for kinase activity, and receptor coupling and CheW binding, respectively, are well conserved among all of the polypeptides.

A diagram of the *Synechocystis* putative TaxD polypeptides is shown in Fig. 2*B*. All three TaxD polypeptides have C-termini with strong similarity to the canonical signaling domain of methyl-accepting chemoreceptors (30–35% identity, 50–60% similarity) and contain the highly conserved signaling domain, known to be important for interactions of methyl-accepting chemoreceptors with both CheA and CheW (28–30). TaxD′ is a truncated version of TaxD1, containing only a portion of the C terminus signaling domain. The N-terminal domains of the TaxD polypeptides, which carry sensing specific information, are significantly different. The two putative transmembrane helices are positioned differently in each of the polypeptides, such that each one has a variable region that is probably intracellular; TaxD2 may also have a large periplasmic domain. A putative HAMP domain has been identified in TaxD2, which may be involved in regulating phosphorylation or methylation of homodimeric receptors (31). TaxD1 has two domains (phy1 and phy2) that are similar to chromophore-binding domains of plant and bacterial phytochromes (Fig. 3) (27, 32). The phy1 domain of TaxD1 does not have the conserved cysteine residue that is chromophorylated in plant phytochromes but does contain a histidine that may bind a

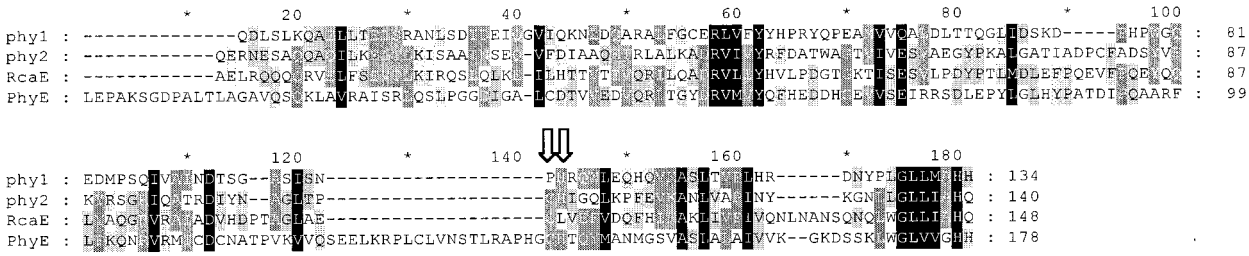

Fig. 3. Comparison of phytochrome-like domains of TaxD1 (phy1 and phy2) with chromophore-binding domain of phytochrome E of *Arabidopsis thaliana* (PhyE, 181–358) and RcaE (89–236) of *Fremyella diplosiphon*. phy1 (210–343) and phy2 (376–515) are shown on lines 1 and 2, respectively. Arrows indicate conserved cysteine and histidine residues. Black boxes indicate identical or conserved residues in all four sequences, whereas dark gray and light gray boxes represent identical or conserved residues in two or three sequences, respectively.

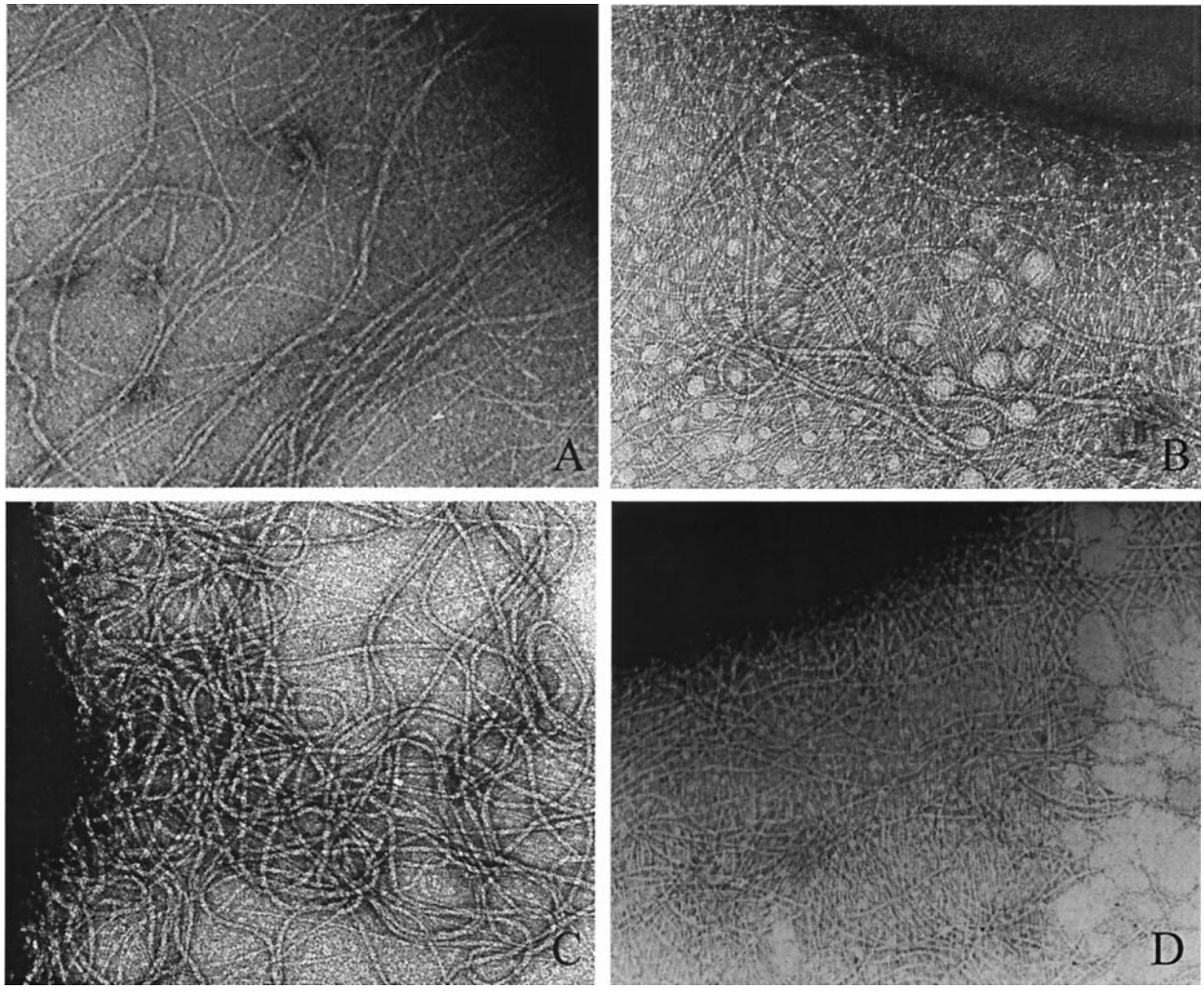

Fig. 4. Transmission electron micrographs of wild-type (*A*), *taxAY1*-3′ (*B*), *taxAY1*-5′ (*C*), and *taxAY3* (*D*) null mutants. Cells were stained with 1% uranyl acetate, and cell edge with pili is shown at a final magnification of 112,500.

chromophore (33). The phy2 domain has the conserved bilin-attached cysteine, as well as the potential chromophore-binding histidine residue of phy1. Phy domains in cyanobacterial and vascular plant phytochromes have also been named GAF domains (in the Pfam database, http://pfam.wustl.edu/) because they are part of a larger family of sequences present in a number of polypeptides including cGMP-specific phosphodiesterases, *Anabaena* adenylate cyclases, and *E. coli* FhlA (34).

In addition to exhibiting aberrant motility, a number of the mutants are abnormal for the extent of piliation (Fig. 4). As shown in Fig. 4*B*, a mutant in *taxAY1* that disrupts only the TaxY-encoding sequence (*taxAY1*-3′) has normal levels of pili and is indistinguishable from wild-type cells. In contrast, a disruption of the *taxAY1*-5′ end (null mutation) causes hyperpiliation (Fig. 4*C*). The hyperpiliation phenotype is very similar to that observed in the *pilT1* mutant and appears to involve elevated production of Tfp but not thin pili. Interestingly, the nonmotile *taxAY3* and *taxD3* mutants exhibit a complete loss of Tfp but not thin pili (Fig. 4*D*). This phenotype resembles that of the *pilA1* mutant (18).

We also examined *taxD* and *taxAY* mutants for expression of *pilA1*, the gene encoding the major pilin subunit of Tfp. As shown in Fig. 5, the *taxAY1*-3′ mutant has normal levels of *pilA1* mRNA, whereas a *taxAY1*-5′ mutant exhibited about a 5-fold increase in the level of *pilA1* mRNA. This increase is in accord with the hyperpiliation phenotype of the mutant and is very similar to the increase in *pilA1* mRNA observed in the nonmotile, hyperpiliated *pilT1* mutant (18). Inactivation of either *taxAY3* or *taxD3* did not alter the level of *pilA1* mRNA, suggesting that the loss of Tfp is not the result of a decrease in *pilA1* mRNA but is possibly because of posttranscriptional control of Tfp biogenesis.

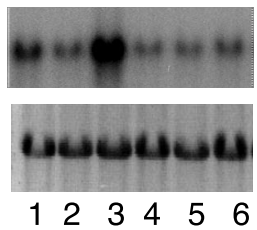

Fig. 5. Northern blot hybridizations. (*Upper*) RNA from wild-type (lane 1), *taxAY1*-3′ (lane 2), *taxAY1*-5′ (lane 3), *taxD1* (lane 4), *taxAY3* (lane 5), and *taxD3* (lane 6) mutants was probed with *pilA1* gene-specific probe. Ten micrograms total RNA were loaded in each lane. (*Lower*) 16S RNA shown as loading control.

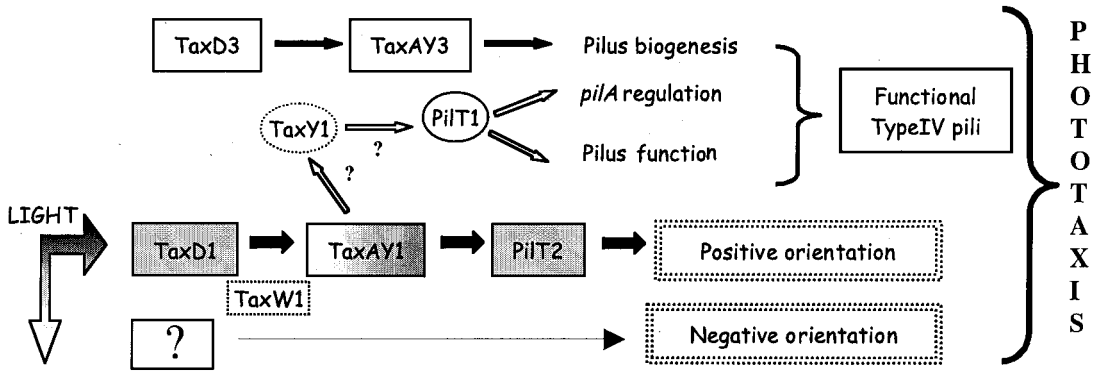

Fig. 6. Regulation of Tfp-mediated motility through chemosensor-like elements. Gray boxes represent mutants that show the inverted response, circles represent nonmotile mutants that have Tfp, and white boxes represent nonmotile mutants lacking Tfp. The black box with a question mark represents a putative photoreceptor that has not yet been identified (see text for details). The circles and boxes with dotted outlines represent elements whose functions have not been tested.

Discussion

We have described *Synechocystis* mutants, generated by *in vitro* transposon mutagenesis, that are aberrant for motility. The mutagenesis technique and screen used in this study offer several advantages. Mutant identification involves a simple visual screen and can be easily modified to examine responses of wild-type and mutant strains to different light qualities and intensities. Based on Southern blot analyses, all of the mutants generated had a single transposon insertion (none had multiple insertions). The screen requires that the cells grow robustly, making the isolation of slow-growing strains, which can resemble nonmotile mutants, unlikely. Because the entire *Synechocystis* genome has been sequenced, identifying the altered gene is easy. Finally, the phenotype of any mutant identified by the screen can be confirmed by targeting specific mutations.

Characterization of 50 mutants yielded 15 strains defective for genes encoding Che-like components in the *Tax1* and *Tax3* loci. Interestingly, all three *taxA* genes have 3′ ends encoding domains with high similarity to CheY response regulators. *taxAY* gene fusions are also present on the genomes of *P. aeruginosa*, *M. xanthus*, and *Rhodospirillum centenum* (35, 36). The three *taxAY* genes of *Synechocystis* encode typical class II histidine kinases (37, 38), although there are some interesting variations among these polypeptides. TaxAY1 has a duplication of the P1 and P2 domains, which is unique among class II histidine kinases, and suggests that there may be more than one site on this polypeptide that undergoes phosphorylation and that this polypeptide may serve multiple roles in regulating phototaxis. Furthermore, there is a unique proline- and glutamine-rich linker region that connects P2 to the dimerization domain, which may facilitate protein–protein interactions or bending.

In addition to the TaxY domains of TaxAY polypeptides, there are three separate, putative TaxY polypeptides encoded in the *Tax* loci. These, in addition to the TaxY domains associated with C-termini of the putative TaxP polypeptides, brings the total number of CheY-like sequences encoded by the *Tax* loci to ten. This raises obvious questions concerning the roles of the several TaxY regulatory domains in the signaling pathways. It has been suggested that multiple CheY elements can serve as sinks for phosphate being transferred among the signal transduction elements, which may obviate the need for a specific phosphatase in the control of taxis responses (39, 40). Interestingly, no gene encoding a CheZ-like phosphatase has been identified on the *Synechocystis* genome.

There are at least three *taxD*-like genes on the *Synechocystis* genome. The *taxD1* mutant exhibited an inverted response, suggesting that (*i*) the mutant colony still responds to directional light, but its response is inverted with respect to wild-type cells, or that (*ii*) the response of the mutant has been sensitized to light, exhibiting a photophobic response even in low intensity light. Hence, TaxD1 is required for forward motility, and when it or other components of this pathway are missing, the default pathway (inverted response) is unmasked. If TaxD1 plays a photosensing role in taxis (as suggested by the phytochrome-like domains at its N terminus), it must be involved in orienting cells with respect to the light direction. However, there is likely to be a second photoreceptor that interfaces with the phototaxis machinery because the cells are still orienting with respect to light direction, but in the inverted orientation (Fig. 6). Interestingly, the inverted response observed in the *taxD1* mutant is most prominent when the cells are exposed to red light (D.B. and A.R.G., unpublished data), suggesting the involvement of another phytochrome-like photoreceptor in phototaxis. Recently, bacterial phytochrome-like molecules have been associated with a number of different light-dependent processes including phototaxis in *Synechocystis* (41–44). Furthermore, there are other Che-like polypeptides involved in light-responsive motility. HtrI and HtrII are Che-like signaling molecules that interact with the rhodopsin-based photoreceptors SRI and SRII, respectively, to control flagellar-based motility in halobacteria (45).

The *taxD3* and *taxAY3* mutants are nonmotile, suggesting that the *Tax1* and *Tax3* loci encode elements of independent pathways, both of which are required for phototaxis. EM data demonstrate that both *taxD3* and *taxAY3* mutants lack Tfp, although levels of *pilA1* mRNA are normal. This suggests that TaxD3 and TaxAY3 are required for Tfp biogenesis at a posttranscriptional level, although the exact roles of these regulatory elements in pilus biogenesis and the signals that modulate the activities of this pathway are not known.

We have attempted to synthesize motility phenotypes, EM data, and information concerning expression of *pilA1* in mutant and wild-type cells into a preliminary, speculative model that describes the control of phototaxis by Tax proteins (Fig. 6). In this model, the phy domains of TaxD1 bind to linear tetrapyrrole chromophores and the holoprotein absorbs light. This putative photoreceptor enables the cells to sense the direction and/or intensity of light, which establishes directional movement. Depending on light conditions, TaxD1 may interact with TaxAY1, perhaps via the scaffold molecule TaxW1. This light-sensitized interaction may promote autophosphorylation of TaxAY1 at the conserved histidine residue of the H box, which is followed by phosphorylation of the fused CheY-like domain. This phosphorylation cascade may ultimately read to PilT2, resulting in positive orientation of the cells with respect to the direction of illumination. Mutants null for TaxD1, the CheY-like domain of TaxAY1, and PilT2 (18) exhibit the inverted response. Hence, all

of these polypeptides are absolutely required for positive phototaxis. However, we have also observed that a *taxAY1* null mutant is nonmotile and shows hyperpiliation and elevated expression of *pilA1*. These phenotypes are identical to those exhibited by the *pilT1* mutant (18). Hence, we suggest that TaxAY1 is multifunctional and that its P1′–P2′ and/or P1–P2 domains read to PilT1, possibly through the mobile TaxY1 polypeptide. PilT1, in turn, is critical for pilus function and for controlling expression of the *pilA1* gene. The elevated *pilA1* mRNA levels in the *taxAY1* null mutant may be an indirect effect of the lesion; when cells assemble nonfunctional pili, the *pilA1* gene may become derepressed. Hence, the bifurcated pathway for light regulation may control both the direction of motility (through the PilT2 branch) as well as the function and regulation of pilus levels through the PilT1 branch.

Our results indicate that *Tax3* genes may be required for Tfp biogenesis, although no mechanistic aspects of this involvement are known. We have placed TaxD3 and TaxAY3 on a pathway, independent of Tax1 polypeptides, that is critical for Tfp biogenesis. It is striking that the conserved histidine residue presumed to be autophosphorylated in the TaxAY1 and TaxAY2 is absent in TaxAY3. So far, there have been no reports indicating the involvement of chemotaxis components in flagellar biosynthesis. However, there are now several reports suggesting that polypeptides of chemosensing pathways in *E. coli* are arranged in large, localized clusters (46, 47). Assembly specifically requires chemosensors, dimeric CheA, as well as CheW (47–49), although this has not been evaluated in cyanobacteria. Tfp biogenesis may be dependent on the correct assembly of the chemosensory complex. Clustering of chemosensors and perhaps Tfp may allow for (*i*) global receptor methylation and integration of diverse environmental signals, (*ii*) an increase in the efficiency of transmitting signals to the motor apparatus, and (*iii*) signal amplification (29, 50).

The model presented above is based on limited data; more information must be incorporated into the model to clarify the role of some of the signaling components. For example, arrows have been drawn directly from TaxAY1 to PilT2 and from TaxAY1 to TaxY1 and PilT1; there is no evidence at this point to suggest that these interactions are direct. However, the model provides a framework for designing experiments to test the validity of the regulatory events proposed and to precisely define circuits involved in controlling both the biosynthesis and function of Tfp.

We have benefited from the excellent technical assistance of Nafisa Ghori, Glenn Ford, and Erin Desing. This work was supported in part by National Science Foundation Grant MCB 9727836 (to A.R.G.). This is Carnegie Institution of Washington publication number 1475.

1. Spormann, A. (1999) *Microbiol. Mol. Biol. Rev.* **63,** 621–641.
2. Youderian, P. (1998) *Curr. Biol.* **8,** R408–R411.
3. Strom, M. S. & Lory, S. (1993) *Annu. Rev. Microbiol.* **47,** 565–596.
4. Merz, A. J., So, M. & Sheetz, M. P. (2000) *Nature (London)* **407,** 98–102.
5. Dubnau, D. (1997) *Gene* **192,** 191–198.
6. Russel, M. (1998) *J. Mol. Biol.* **279,** 485–499.
7. Tennent, J. M. & Mattick, J. S. (1994) in *Fimbriae*, ed. Klemm, P. (CRC, Boca Raton, FL), pp. 127–146.
8. Bieber, D., Ramer, S. W., Wu, C. Y., Murray, W. J., Tobe, T., Fernandez, R. & Schoolnik, G. K. (1998) *Science* **280,** 2114–2118.
9. Semmler, A. B., Whitchurch, C. B. & Mattick, J. S. (1999) *Microbiology* **145,** 2863–2873.
10. Wall, D. & Kaiser, D. (1999) *Mol. Microbiol.* **32,** 1–10.
11. Cho, K., Treuner-Lange, A., O'Connor, K. A. & Zusman, D. R. (2000) *J. Bacteriol.* **182,** 6614–6621.
12. Yang, Z., Geng, Y., Xu, D., Kaplan, H. B. & Shi, W. (1998) *Mol. Microbiol.* **30,** 1123–1130.
13. Ward, M. J. & Zusman, D. R. (1999) *Curr. Opin. Microbiol.* **2,** 624–629.
14. Hader, D. P. (1987) in *The Cyanobacteria*, eds. Fay, P. & VanBaalen, C. (Elsevier, New York), pp. 325–346.
15. Hoiczyk, E. (2000) *Arch. Microbiol.* **174,** 11–17.
16. Hoiczyk, E. & Baumeister, W. (1997) *Mol. Microbiol.* **26,** 699–708.
17. Brahamsha, B. (1996) *Proc. Natl. Acad. Sci. USA* **93,** 6504–6509.
18. Bhaya, D., Bianco, N. R., Bryant, D. & Grossman, A. (2000) *Mol. Microbiol.* **37,** 941–951.
19. Armitage, J. P. (1998) in *Microbial Responses to Light and Time*, ed. Caddick, M. X. (Cambridge Univ. Press, Cambridge, U.K.), pp. 33–55.
20. Sun, H., Zusman, D. R. & Shi, W. (2000) *Curr. Biol.* **10,** 1143–1146.
21. Sambrook, J., Fritsch, E. F. & Maniatis, T. (1989) *Molecular Cloning: A Laboratory Manual* (Cold Spring Harbor Lab. Press, Plainview, NY).
22. Bhaya, D., Watanabe, N., Ogawa, T. & Grossman, A. R. (1999) *Proc. Natl. Acad. Sci. USA* **96,** 3188–3193.
23. Kehoe, D. & Grossman, A. (1999) *Methods Enzymol.* **297,** 279–290.
24. Ward, M. J., Lew, H. & Zusman, D. R. (2000) *Mol. Microbiol.* **37,** 1357–1371.
25. Ward, M. J., Mok, K. C., Astling, D. P., Lew, H. & Zusman, D. R. (1998) *J. Bacteriol.* **180,** 5697–5703.
26. Liang, J., Scappino, L. & Haselkorn, R. (1992) *Proc. Natl. Acad. Sci. USA* **89,** 5655–5659.
27. Kehoe, D. M. & Grossman, A. R. (1996) *Science* **273,** 1409–1412.
28. Levit, M., Liu, Y. & Stock, J. (1998) *Mol. Microbiol.* **30,** 459–466.
29. Stock, J. & Levit, N. (2000) *Curr. Biol.* **10,** R11–R14.
30. Falke, J. J., Bass, R. B., Butler, S. L., Chervitz, S. A. & Danielson, M. A. (1997) *Annu. Rev. Cell Dev. Biol.* **13,** 457–512.
31. Aravind, L. & Ponting, C. P. (1999) *FEMS Microbiol. Lett.* **176,** 111–116.
32. Vierstra, R. D. & Davis, S. J. (2000) *Semin. Cell Div. Biol.* **11,** 511–521.
33. Davis, S. J., Vener, A. V. & Vierstra, R. D. (1999) *Science* **286,** 2517–2520.
34. Aravind, L. & Ponting, C. P. (1997) *Trends Biochem. Sci.* **22,** 458–459.
35. McCleary, W. R. & Zusman, D. R. (1990) *Proc. Natl. Acad. Sci. USA* **87,** 5898–5902.
36. Jiang, Z.-Y. & Bauer, C. E. (1997) *J. Bacteriol.* **179,** 5712–5719.
37. Dutta, R., Qin, L. & Inouye, M. (1999) *Mol. Microbiol.* **34,** 633–640.
38. Bilwes, A. M., Alex, L. A., Crane, B. R. & Simon, M. I. (1999) *Cell* **96,** 131–142.
39. Sourjik, V. & Schmitt, R. (1998) *Biochemistry* **37,** 2327–2335.
40. Shah, D. S. H., Porter, S. L., Martin, A. C., Hamblin, P. A. & Armitage, J. P. (2000) *EMBO J.* **19,** 4601–4613.
41. Yeh, K. C., Wu, S.-H., Murphy, J. T. & Lagarias, J. C. (1997) *Science* **277,** 1505–1508.
42. Zhulin, I. B. (2000) *J. Mol. Microbiol. Biotechnol.* **2,** 491–493.
43. Jiang, Z.-Y., Swem, L. R., Rushing, B. G., Devanathan, S., Tollin, G. & Bauer, C. E. (1999) *Science* **285,** 406–409.
44. Yoshihara, S., Suzuki, F., Fujita, H., Geng, X. & Ikeuchi, M. (2000) *Plant Cell Physiol.* **41,** 1299–1304.
45. Hoff, W. D., Jung, K.-H. & Spudich, J. L. (1997) *Annu. Rev. Biophys. Biomol. Struct.* **26,** 223–258.
46. Maddock, J. R. & Shapiro, L. (1993) *Science* **259,** 1717–1723.
47. Sourjik, V. & Berg, H. C. (2000) *Mol. Microbiol.* **37,** 740–751.
48. Skidmore, J., Ellefson, D. D., McNamara, B. P., Couto, M. M. P., Wolfe, A. J. & Maddock, J. R. (2000) *J. Bacteriol.* **182,** 967–973.
49. Wadhams, G. H., Martin, A. C. & Armitage, J. P. (2000) *Mol. Microbiol.* **36,** 1222–1233.
50. Duke, T. A. & Bray, D. (1999) *Proc. Natl. Acad. Sci. USA* **96,** 10104–10108.